

Optimized Green Synthesis of *Manilkara zapota* Capped Silver Nanoparticles and Their Antimicrobial Application Through Formulation of Nano-gel Systems

Sonia Parashar, Munish Garg 

Department of Pharmaceutical Sciences, Maharshi Dayanand University, Rohtak, India

 Corresponding author. E-mail: munishgarg@mdurohtak.ac.in

Received: May 25, 2022; **Revised:** Jan. 23, 2023; **Accepted:** May 5, 2023

Citation: S. Parashar, M. Garg. Optimized green synthesis of *Manilkara zapota* capped silver nanoparticles and their antimicrobial application through formulation of nano-gel systems. *Nano Biomedicine and Engineering*, 2023, 15(3): 262–277.

<http://doi.org/10.26599/NBE.2023.9290020>

Abstract

The present study is based on optimized green synthesis of silver nanoparticles (AgNPs) using *Manilkara zapota* fruit extract, formulation of topical gels, and evaluation for their antimicrobial properties. The results reveal that a reaction temperature of 35 °C and a reaction time of 11 h are the optimum conditions to get spherical AgNPs with a particle size of 100.7 nm and a zeta potential of –26.7 mV. The synthesized AgNPs formulated as topical gels demonstrate a broad-spectrum antimicrobial activity against *Escherichia coli*, *Staphylococcus aureus*, *Pseudomonas aeruginosa*, and *Aspergillus niger* in comparison to the 0.2% (mass fraction) silver nitrate marketed formulation. The AgNPs loaded gels seem promising and could lead to a useful alternative for treating pathogenic infections.

Keywords: silver nanoparticles; green synthesis; optimization; agar well diffusion; topical gel; antimicrobial

Introduction

Resistance to microbes seems to be an inescapable side effect of almost every new antimicrobial agent, and it is recognized as a big problem in the treatment of pathogenic infections in hospitals as well as community [1]. Substantial efforts have been made and continuous research is still going on in the field of new antimicrobial agents to deal with such resistant microbes. Nanotechnology is a promising and rapidly growing science with numerous applications, including food packaging materials,

personal care items, and therapeutic drug delivery systems to improve medical treatments [2]. Nanoparticles have a high surface-to-volume ratio, allowing for strong interactions at therapeutic locations while their small size allows for passage through biological membranes [3]. Among different types of nanoparticles, silver nanoparticles (AgNPs) are extensively studied as effective antimicrobial agents against a broad range of fungi, bacteria, and viruses [4]. Apart from antimicrobial activity, AgNPs also possess other important applications like catalysis [5], municipal sewage treatment [6], and crop protection [7]. Different physical and chemical

approaches have been used for the synthesis of AgNPs, but they all suffer from a number of drawbacks: being toxic, expensive, and difficult to synthesize in large quantity. A new strategy known as the green synthesis has been put in place to overcome these obstacles [8]. Biocompatible and environmentally acceptable components such as animal chitin, microbe, crude extract from seed, and leaves and bark of plants are used in the green technique [9]. Plant metabolites like flavonoids, alkaloids, tannins, phenolic acids, and saponins are primarily involved in the reduction of Ag^+ to Ag^0 to obtain non-toxic nanosized particles, and also play an effective role in the capping of the synthesized silver nanoparticles [10, 11]. Different mechanisms have been proposed for the antimicrobial effects of AgNPs. AgNPs have been shown to act as strong adsorbents, disrupting metabolic pathways of microbes via a variety of mechanisms (e.g., the stoppage of electron transfer events and the generation of reactive oxygen species) [12, 13]. AgNPs may interact with the bacterial membrane, causing damage to the membrane and, as a result, bacterial death. AgNPs would first collect on bacterial membrane's surface, then penetrate within the cell, causing altered permeability of the membrane and significant damage to the membrane [14]. Another recent mechanistic study reveals that AgNPs' capacity to damage the bacterial cell wall may be due to their interaction with the cell wall's peptidoglycan layer [15].

Gels are biphasic swelling networks that have both the cohesive and diffusive transport properties of solids and liquids. Gels, unlike ointments and creams, frequently provide a quick release of the active pharmaceutical ingredient, regardless of the drug's water solubility. They are remarkably biocompatible and have a low risk of inflammation and undesirable reactions. Gels are simple to apply to the skin and do not require removal. Gels for skin application have a variety of appealing characteristics. They have an emollient effect and are thixotropic and non-greasy. Gels are easily spreadable and can be easily wiped out after washing because they are water washable [16]. Gels are semisolid systems made up of either inorganic particle suspensions or big organic molecules that are interpenetrated by a liquid, according to the United States Pharmacopeia (USP) [17].

Carbopol is a carbomer-based synthetic polymer.

Cross-linked carbomer polymers form a microgel structure that can be used in dermatological applications. Because these polymers are anionic in nature, they require neutralization for micro gel construction, which is why organic amines like tri ethanolamine are utilized. It has been employed as a suspending agent, stabilizer, and thickener [18, 19].

In this research, the optimized green synthesis of AgNPs using *Manilkara zapota* fruit extract has been accounted. *M. zapota* (MZ) fruits are rich in polyphenols like quercitrin, dihydromyricetin, methyl chlorogenate, myricitrin, (+)-gallic acid, (-)-epicatechin, (+)-catechin, and gallic acid and the antimicrobial potential of various parts of *M. zapota* has been reported in a number of studies [20]. Several studies have reported the role of polyphenols in the biosynthesis of silver nanoparticles [21–24]. Moreover, no efforts have been made till date for the optimized synthesis of silver nanoparticles using *M. zapota* fruit extract. The present study aimed to synthesize AgNPs using *M. zapota* fruit extract by optimization of reaction parameters like reaction time and temperature for efficient production of AgNPs using central composite design. The optimized AgNPs were incorporated into two carbopol based topical gels and evaluated for their *in vitro* antimicrobial potential. The antimicrobial activity of the gels was also compared with that of the marketed formulation containing 0.2% (mass fraction) silver nitrate.

Material and Methods

Material

Chemicals were procured from Loba Chemie and HiMedia, Mumbai, Maharashtra, India and silverex gel containing 0.2% (mass fraction) silver nitrate was procured from Sun Pharmaceutical Industries Ltd. The microbial strains, i.e., *Staphylococcus aureus* (ATCC 6538), *Bacillus subtilis* (ATCC 1272), *Escherichia coli* (ATCC 8739), *Klebsiella pneumoniae* (ATCC 13882), *Pseudomonas aeruginosa* (ATCC 25619), *Candida albicans* (ATCC 10231), and *Aspergillus niger* (ATCC 6275), were collected from "Enzyme & fermentation technology Lab", Department of Microbiology, M.D.U, Rohtak.

Preparation of silver nitrate solution

By dissolving 0.017 g of AgNO_3 in 100 mL of

Milli-Q water, a 1 mmol/L aqueous solution of AgNO_3 was prepared and used for the synthesis of silver nanoparticles.

Preparation of extract

M. zapota fruits were thoroughly washed, first with running tap water and then with Milli-Q water. The washed fruits were crushed after being sliced into small pieces. In 200 mL of Milli-Q water, 40 g of crushed material was added. The resulting mixture was stirred on a magnetic stirrer for 20 min before being filtered through Whatman filter paper No. 1; the filtrate was used for AgNP synthesis.

Green synthesis of AgNPs using *M. zapota* fruit extract

The prepared extract of *M. zapota* was slowly added to 1 mmol/L aqueous AgNO_3 solution in a ratio of 1:5. The mixture was stirred for 10 min at 2 000 r/min on a magnetic stirrer. Within 5 min, the reaction mixture turned yellowish brown, and the colour progressed to deep brown over time. The resulting AgNPs were centrifuged at 15 000 r/min for 20 min before being washed several times with Milli-Q water. A lyophilizer was used to dry the purified nanoparticles [25].

Optimization and evaluation of dependent variables

Design of experiments (DOE) and data analysis were used to optimize the synthesis parameters of AgNPs

using the statistical software Design-Expert (version 13). The DOE suggested 13 experimental runs based on two variables at two levels. Reaction time and reaction temperature were chosen as independent variables. Particle size and zeta potential were the dependent variables. The level of the variable chosen for CCD design is shown in Table 1. The developed model was assessed using statistical methods such as analysis of variance (ANOVA) and the *F*-test. The coefficient of determination, R^2 , was used to express the model equation's quality of fit. Three-dimensional (3D) surface designs and perturbation designs are plotted to demonstrate relationships between responses. Following the development of an appropriate mathematical model, the desirability function was investigated in order to optimize the independent variables.

Synthesis and characterization of the optimized AgNPs

The AgNPs were synthesized at optimum time and temperature conditions and thereafter characterized using ultraviolet–visible (UV–Vis) spectrophotometer (UV-1800 Shimadzu, Japan) within the wavelength range of 200–800 nm using quartz cuvettes of 1 cm path length. The morphological features (shape and size) of the synthesized AgNPs were investigated by transmission electron microscopy (TEM) (Talos F200X TEM for Materials Science) using carbon coated copper grids. Fourier transform infrared (FT-IR) spectroscopic analysis was done to find the

Table 1 Experimental design and results of central composite design

Formulation	Independent factors		Dependent factors	
	Reaction time (X_1)	Reaction temperature (X_2)	Particle size (nm)	Zeta potential (mV)
A1	−1	−1	117.1	−27.4
A2	+1	−1	119.4	−19.4
A3	−1	+1	85.14	−20.6
A4	+1	+1	70.98	−22.3
A5	−1.414	0	114.9	−25.4
A6	+1.414	0	97.14	−20.6
A7	0	−1.414	121	−24.3
A8	0	+1.414	76.46	−18.1
A9	0	0	108.3	−25.9
A10	0	0	109	−26.1
A11	0	0	105.6	−26.1
A12	0	0	108.1	−26.4
A13	0	0	101.5	−22.9

possible functional groups involved in the reduction and capping of AgNPs using KBr pellets using Bruker Alpha II FT-IR. Size and stability of the particles were evaluated by dynamic light scattering (DLS) using zeta sizer instrument (Malvern Zeta sizer, Nano ZS90) [26–28].

Determination of zone of inhibition, minimum inhibitory concentration (MIC), and minimum bactericidal concentration/minimum fungicidal concentration (MBC/MFC) of the optimized AgNPs

S. aureus (ATCC 6538), *B. subtilis* (ATCC 1272), *E. coli* (ATCC 8739), *K. pneumoniae* (ATCC 13882), and *P. aeruginosa* (ATCC 25619) were grown on tryptone broth and incubated at 37 °C for 24 h. *C. albicans* (ATCC 10231) and *A. niger* (ATCC 6275) spore suspensions were prepared and were grown on potato dextrose broth and incubated for 5–7 days at room temperature. For zone of inhibition study, the *S. aureus*, *B. subtilis*, *E. coli*, *P. aeruginosa*, and *K. pneumoniae* (bacterial strains) were inoculated on Soyabean Casein Digested Agar (SCDA) plates. 20 µL and 10 µL of the samples (synthesized AgNPs and *M. zapota* fruit extract) at a concentration of 5 mg/mL and 20 µL of the standard-ciprofloxacin at a concentration of 0.1 mg/mL were added to 5 mm wells on agar plates. *C. albicans* and *A. niger* were inoculated on potato dextrose agar (PDA) plates. 20 µL and 10 µL of the samples (synthesized AgNPs and *M. zapota* fruit extract) at a concentration of 5 mg/mL and 20 µL of the standard-itraconazole at a concentration of 1 mg/mL were added to 5 mm wells on PDA plates. The treated plates were incubated for 24 h at 37 °C (for bacteria) and at room temperature for 2–3 days (for fungi). After incubation period, the treated plates were looked for inhibition zones around the wells. For MIC value determination, test samples/standard of different test concentration were mixed with 10 µL inoculum in 96-well plates (100 µL/well). For control: Tryptone broth without drug was mixed with 10 µL inoculum in 96-well plates. Treated plates were incubated at 37 °C for bacteria and 27 °C for fungi for 24 h. After incubation, the optical density (OD) was measured at 590 nm using a plate reader. To observe colour change, resazurin was added to all wells (30 µL in each well) and incubated for 2–4 h. Columns with no colour change (blue) at the end of the incubation gave MIC value. Purple-blue colored

resazurin was reduced to pink-colorless resorufin after being metabolized by active bacterial cells. Turbidity implied microbial growth, while MIC was the lowest concentration at which no visible cell metabolism occurred. The MIC dilution and at least two-four of the more concentrated test product dilutions were applied (0.1 mL) to SCDA plates and incubated at 37 °C for 24 h to determine the MBC. The dilution concentration that produced no growth was recorded as the MBC. To determine the MFC, the MIC dilution and at least two-four of the more concentrated test product dilutions were added (0.1 mL) to PDA plates and incubated for 5–7 days at room temperature and enumerated to determine viability of cells (colony forming unit (CFU)/mL). The dilution concentration that produced no growth was recorded as the MFC [29].

Drug-excipient compatibility studies

Formulation of the gels was preceded by preformulation studies to look for any possible interactions between the AgNPs and carbopol. FT-IR spectral studies were done to establish compatibility between carbopol and AgNPs using FT-IR spectrophotometer (Bruker Alpha II).

Formulation of AgNPs incorporated gels

Two gel formulations (A and C) of the synthesized AgNPs (optimized batch) were prepared using carbopol 934 (A) and 940 (C) as gelling agents by cold mechanical method. A colloidal suspension of the AgNPs (mass fraction of 0.055%) was prepared and 3% carbopol was slowly added to it with continuously stirring followed by addition of a drop of triethanolamine. The prepared gels were packed properly in wide mouthed containers and stored in cool and dark place [30].

Evaluation of AgNPs gels

The prepared gels were evaluated for their physicochemical parameters like color, appearance, homogeneity, pH, viscosity, spreadability, zeta potential, extrudability, rheological parameters, *in vitro* diffusion, release kinetic studies, and stability.

Color, appearance, and homogeneity

The formulations were checked for their color, appearance, and homogeneity by visual inspection [31].

pH and viscosity

Digital pH meter (PR-11, Sartorius) was used to

evaluate the gels for their pH. For pH measurement, 1 g of the AgNPs gel was mixed with 100 mL of water and stored at 4 °C for 2 h. All of the measures were done three times and the averages were recorded [32]. The viscosity of the gel formulations was evaluated using a Brookfield viscometer (DV II RVTDV-II) using spindle No. 63 at 200 r/min. Before taking measurements, the gel samples were allowed to settle for 30 min at (25 ± 1) °C.

Spreadability

For spreadability determination of gel formulations, the spreading diameter of 1 g of gel sandwiched between two horizontal plates after 1 min was measured. The upper plate's typical mass was 125 g [33].

Zeta potential

All the formulations were analyzed for their zeta potential using zeta sizer instrument (Malvern Zeta sizer, Nano ZS90).

Extrudability

The method used to assess gel extrudability was based on the amount of gel extruded from a tube as a percentage when a given load was applied. The understudy formulation was placed in a collapsible tube with a 5 mm tip aperture. A mass of 50 g was placed at the bottom of the tube to release gel through the hole. To determine extrudability, the amount of gels extruded via the tip was weighed, calculated, and reported [34].

Rheological studies

The rheological parameters are an important aspect for observing the applicability of gels. The gels should be of such a consistency that it should not be too viscous or too runny while squeezing out from the container. Steady shear properties and frequency sweep test were studied with the help of a rheometer (Anton Paar MCR 102) using cone and plate geometry. The approach given by Sandhu et al. was used to calculate dynamic rheological parameters [35]. The approach provided by Park et al. with minor adjustments was used to determine steady shear characteristics [36]. To define the variation in the samples' rheological properties under steady shear, the data was fitted to the power law:

$$\sigma = K\gamma^n \quad (1)$$

where σ denotes shear stress (Pa), γ denotes the shear

rate in s^{-1} , K denotes the consistency index ($Pa \cdot s^n$), and n denotes the flow behavior index, which was calculated by linear regression of the square roots of shear rate–shear stress data.

Steady shear properties

For the easy application of gels from the tube, they should exhibit a pseudoplastic/non-Newtonian behavior, where an increase in shear rate decreases the viscosity of the gel. This is termed as shear thinning behavior. At the same time, gels must possess a high viscosity so as to stay at the site of application [37]. Such a behavior can be predicted by studying steady shear properties. The gel formulations were analyzed for these properties using a rheometer (Anton Paar MCR 102) by applying shear at the rate of 0 to 100 s^{-1} at 25 °C. K , yield stress (τ), n , and R^2 were noted.

Frequency sweep test

It was performed using a rheometer (Anton Paar MCR 102) by increasing the angular frequency at a rate of 0.1 to 100 rad/s. A graph of elastic modulus (G') vs. viscous modulus (G'') against angular frequency was obtained.

In vitro diffusion

The release of AgNPs from carbopol 940 and carbopol 934 gels *in vitro* was investigated. 1 g of AgNPs incorporated into carbopol gel was precisely weighed and inserted into a dialysis membrane as a donor compartment. As the release medium, the bag was submerged in a beaker (receptor compartment) filled with 20 mL de-ionized water maintained at pH = 6. A magnetic stirrer was used to agitate the receptor compartment at a constant speed of 100 r/min. The temperature was kept at (37 ± 1) °C. 2 mL of aliquots were removed and replaced with fresh media at intervals of 0, 0.5, 1, 2, 3, 4, 5, 6, 7, and 8 h. To determine the amount of silver nanoparticles present in the collected samples, the absorbance was measured at 430 nm [38].

Release kinetic studies

To characterize the overall release of the medication from dosage forms, a variety of kinetic models existed. Because changes in a formulation's quality and quantity might alter drug release and *in vivo* performance, it's always a good idea to design approaches that reduce the requirement for bio-studies and so make product development easier [39].

The data from the AgNPs release studies from gel formulations was fitted to various kinetic equations, including zero order, first order, Higuchi model, and Korsmeyer-Peppas model.

Stability studies

The gel formulations were packed in collapsible tubes and stored for 6 months at room temperature. During this period, the samples were analyzed for their color, homogeneity, pH, and zeta potential by earlier stated procedures.

Antimicrobial activity of the gels

The prepared formulations (A and C) were evaluated for their antimicrobial potential against different bacteria (*S. aureus*, *B. subtilis*, *E. coli*, *K. pneumoniae*, and *P. aeruginosa*) and fungi (*A. niger* and *C. albicans*) and compared with marketed formulation silverex M (silver nitrate 0.2% mass fraction). The bacterial strains were grown on tryptone broth and incubated for 24 h at 37 °C. Spore suspension of the fungal strains was prepared and grown on potato dextrose broth and incubated for 5–7 days at room temperature. The bacterial strains were inoculated on SCDA plates and the fungi were inoculated on PDA plates. 10 µL of AgNPs gel A and C (0.055% mass fraction) and marketed formulation silverex M containing 0.2% silver nitrate were added to the 5 mm wells on agar plates and PDA plates for bacteria and fungi, respectively. The treated plates were incubated for 24 h at 37 °C for bacteria and at room temperature for 2–3 days for fungi. After incubation, the treated plates were observed for inhibition zones around the wells and compared with the marketed gel [26].

Results and Discussion

Green synthesis of AgNPs using *M. zapota* fruit extract

M. zapota fruit extract was added to 1 mmol/L AgNO₃ solution in a ratio of 1:5. Initially, AgNO₃ was colourless and after the addition of the extract to it, the reaction mixture turned yellowish brown almost immediately, and the colour further deepened to brown after 30 min. Because of the characteristic surface plasmon vibrations, AgNPs in aqueous solution have a yellowish brown color [40]. The phytochemicals present in the extract could have reduced the silver ions. Polyphenols (quercetin, methyl chlorogenate,

dihydromyricetin, (+)-gallo catechin, myricitrin, (+)-catechin, (–)-epicatechin, and gallic acid) are abundant in *M. zapota* [41]. Figure 1 shows the AgNPs synthesis by an eco-friendly approach using *M. zapota* fruit extract and incorporation of the synthesized nanoparticles into a carbopol based gel.

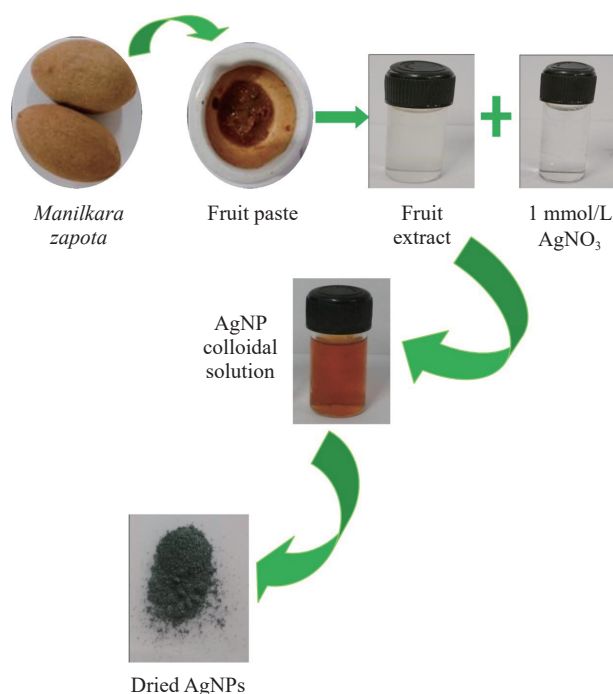


Fig. 1 AgNPs synthesis by an eco-friendly approach using *M. zapota* fruit extract and incorporation of the synthesized nanoparticles into a carbopol based gel.

Optimization and evaluation of dependent variables

The statistical process optimization of AgNPs production using response surface methodology (RSM) was used to identify the most prominent interaction between significant parameters in order to produce the smallest sized AgNPs with the greatest stability. A central composite experimental design with two independent variables at two distinct levels was used to investigate their effects on the dependent variables. Table 1 displays the transformed values of all batches, as well as their responses. Using mathematical relationships obtained from the statistical package, the relationship between dependent and independent variables was established. The polynomial equations obtained were as follows:

$$Y_1 = 106.50 - 4.62A - 17.92B - 4.11AB - 1.29A^2 - 4.94B^2 \quad (2)$$

$$Y_2 = -25.48 + 1.60A + 1.62B - 2.35AB + 1.14A^2 + 2.04B^2 \quad (3)$$

where Y_1 represents the response, i.e., particle size, Y_2 represents the response zeta potential, and A and B are variables.

Following consideration of the numerical sign and extent of the coefficient, polynomial equations can be used to make inferences. The values of correlation coefficient (R^2) for particle size and zeta potential were found to be 0.96 and 0.89, respectively, indicating a good fit. Negative values of coefficients A and B in Eq. (2) indicate an antagonistic effect of this variable on size. Positive values for both the coefficients A and B in Eq. (3) indicate a favorable effect of these two variables on zeta potential.

ANOVA analysis report

The significance and suitability of the model were evaluated using ANOVA. Table 2 contains statistical information such as standard error, sum of squares, F -ratio, and P -value. As shown in Table 2, a P -value of 0.05 for the independent variables and their interaction in ANOVA indicates that the corresponding factors have a significant effect on particle size and zeta potential. 3D reaction surface plots show a variety of representations in each reaction as the two components are changed from a lower to a higher amount. It provides a 3D bend of the adjustment at various component levels. It also provides a range of outline focuses based on the expected response esteem. Figures 2–5 show the 3D response surface plots and corresponding contour plots for particle size and zeta potential.

Optimized batch of AgNPs

The optimized batch was selected by numerical optimization with desirability function value closer to

1. The optimum conditions of synthesizing AgNPs came out to be 35 °C and 11 h. It also indicated predicted response for synthesized AgNPs having particle size 113.9 nm and zeta potential of -25.28 mV. Further, the validation studies were performed on the optimized AgNPs and responses were evaluated. The observed values of responses for the synthesized AgNPs were found as particle size 100.7 nm and zeta potential -26.7 mV. The observed values obtained were quite closer to the predicted response (i.e., within prediction error $\pm 10\%$) and goodness of fit of the selected design and mathematical model.

Characterization of the optimized AgNPs

A clear surface plasmon resonance band centered at around 430 nm can be seen in UV–Vis spectra of AgNPs (Fig. 6), which is assumed to be an indication of spherical nanoparticles. It is well known that AgNPs in aqueous solution have a yellowish brown color due to plasmonic nanoparticles [39]. Polyphenols ((–)-epicatechin, quercetin, (+)-catechin, dihydromyricetin, myricitrin, methyl chlorogenate, (+)-gallic acid, and gallic acid) are abundant in *M. zapota*. It was assumed that the phytochemicals present in the extract could have reduced the silver ions [40]. The appearance of characteristic diffraction peaks at 38.14° (111), 44.41° (200), 64.54° (220), and 77.53° (311) as seen in Fig. 7 can be indexed to face center cubic (fcc) structure of silver. The X-ray diffraction (XRD) pattern clearly revealed that the nanoparticles formed are crystalline in nature. The nanoparticles were smaller than 50 nm in size and spherical in shape, according to TEM observations (Fig. 8). The AgNPs were capped by biomolecules

Table 2 Summary of results of ANOVA

Source	DF	Zeta potential				Particle size			
		SS	MS	F	P	SS	MS	F	P
A	1	20.44	20.44	12.49	0.0095	170.91	170.91	8.98	0.0200
B	1	21.02	21.02	12.85	0.0089	2569.34	2569.34	134.98	<0.0001
AB	1	22.09	22.09	13.50	0.0079	67.73	67.73	3.56	0.1012
A^2	1	9.04	9.04	5.53	0.0510	11.67	11.67	0.6129	0.4594
B^2	1	28.95	28.95	17.69	0.0040	169.76	169.76	8.92	0.0203
Residual	7	11.45	1.64			133.25	19.04		
Lack of fit	3	3.01	1.00	0.4745	0.7168	95.39	31.80	3.36	0.1362
Pure error	4	8.45	2.11			37.86	9.47		
Cor total	12	109.36				3113.99			

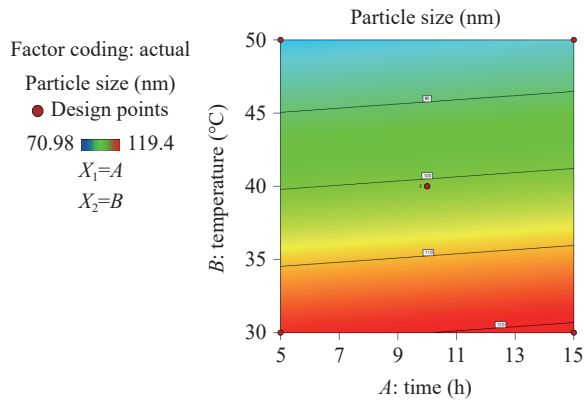


Fig. 2 Contour plot for particle size.

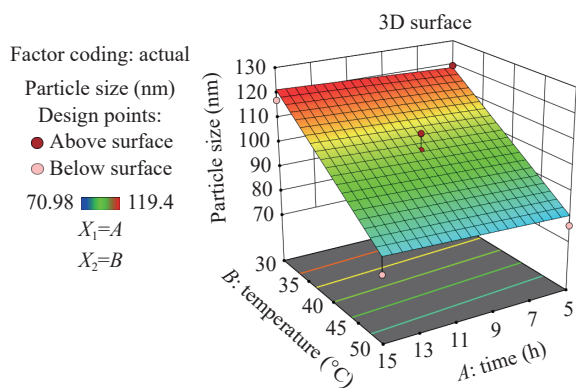


Fig. 3 3D response surface plot for particle size.

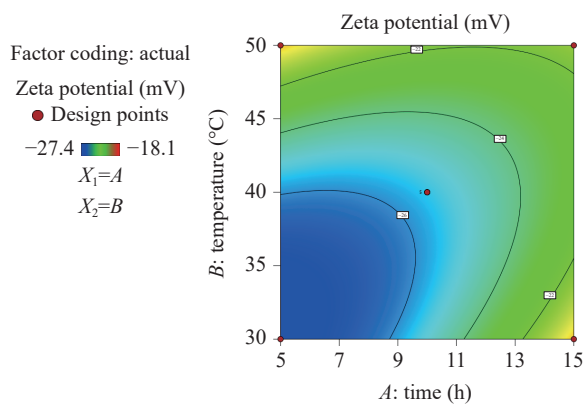


Fig. 4 Contour plot for zeta potential.

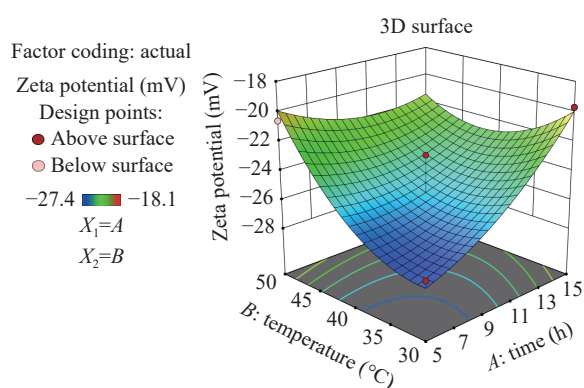


Fig. 5 3D response surface plot for zeta potential.

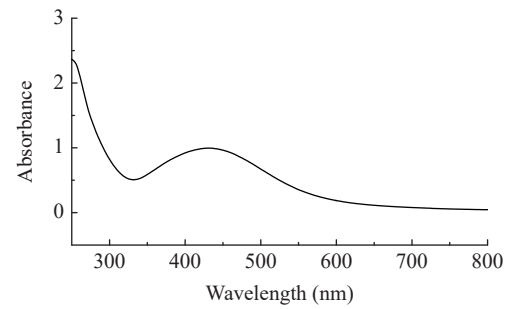


Fig. 6 UV-Vis spectra of optimized AgNPs synthesized from *M. zapota* fruit.

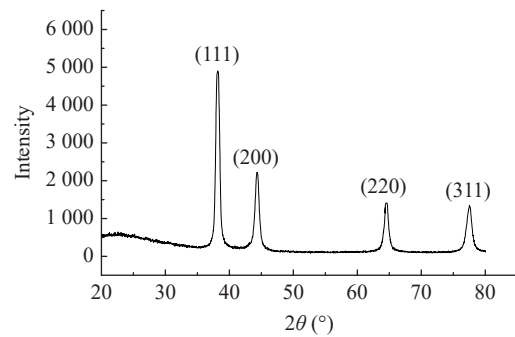


Fig. 7 XRD of the synthesized AgNPs.

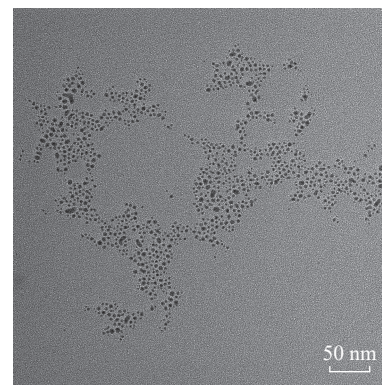


Fig. 8 TEM image of the synthesized AgNPs.

such as phenols, amino acids, aldehyde, carboxylic acid, and others present in the fruit extract, as confirmed by FT-IR peaks (Fig. 9). Tables 3 and 4 depict the functional groups with their transmittance values detected in FT-IR spectra of MZ extract and MZ-AgNPs, respectively. The presence of these functional groups on the AgNPs surface prevents their agglomeration from conferring stability to them. DLS measurements revealed that the AgNPs were found to possess an average size of 100.7 nm (Fig. 10) which was close to that suggested by the software (113.9 nm) for the optimized batch. According to the findings, the measured size of AgNPs using DLS was found to be larger than the TEM measurements. This distinction reveals that DLS measures particle diameter in addition to

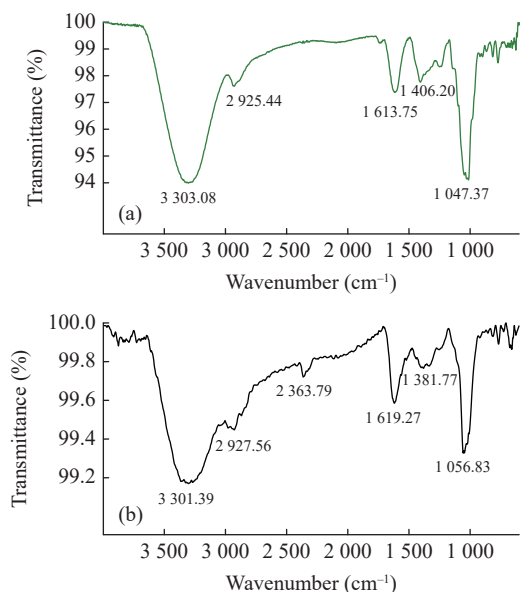


Fig. 9 FT-IR spectra of (a) *M. zapota* fruit extract and (b) *M. zapota* capped AgNPs.

molecules or ions attached to the surface of AgNPs, whereas TEM is based solely on a number base size distribution and is devoid of any capping agent [42].

The particles have reasonably good stability as indicated by a zeta potential value of -26.7 mV (Fig. 11) that was found to be quite close to that suggested by the software (-25.28 mV) for the optimized batch. The polydispersity index (PDI) of the synthesized nanoparticles (0.228) was less than 0.4, indicating that they were almost monodisperse in nature.

Determination of MIC and MBC/MFC of the synthesized AgNPs

The optimized silver nanoparticles and the *M. zapota* fruit extract were evaluated for their activity against *S. aureus*, *B. subtilis*, *E. coli*, *K. pneumonia*, *P. aeruginosa*, *C. albicans*, and *A. niger* by agar-well diffusion method. The zone of inhibition of the nanoparticles ranged between 6 and 15 mm, MIC values ranged between 0.0625 and 0.5 mg/mL, and MBC/MFC value ranged between 0.5 and 0.625 mg/mL, except for *B. subtilis* where no activity was detected for the extract. The results are presented in Table 5. It was observed from the results that the

Table 3 Functional groups with their transmittance values detected in FT-IR spectra of MZ extract

Serial No.	Functional groups	Transmittance (cm ⁻¹)
1	Intermolecular H-bonded —OH group of phenolic compounds	3303.08
2	Stretching frequency of alkanes	2925.44
3	NH bending of amino acids	1613.75
4	Carboxylate group	1406.20
5	C—O group of phenols/alcohols	1047.37

Table 4 Functional groups with their transmittance values detected in FTIR spectra of MZ-AgNPs

Serial No.	Functional groups	Transmittance (cm ⁻¹)
1	Interactions between the extract biomolecules and silver metal	3301.39
2	Stretching frequency of alkanes	2927.56
3	C—O group of phenols/alcohols	1056.83
4	NH bending of amino acids	1619
5	Carboxylate group	1381.77
6	Interaction between the extract and the silver metal	2363.79

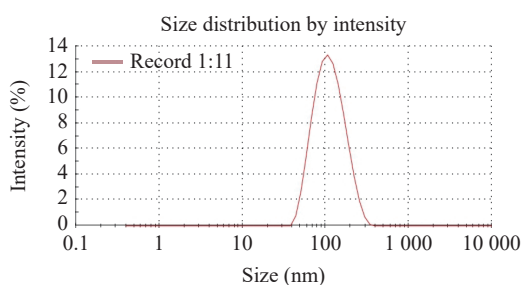


Fig. 10 Particle size of the synthesized AgNPs.

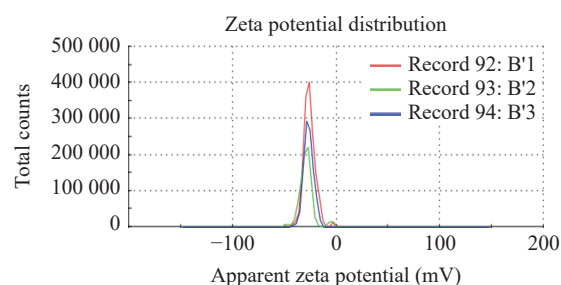


Fig. 11 Zeta potential of the synthesized AgNPs.

Table 5 MIC and MBC/MFC of *M. zapota* extract and *M. zapota* AgNPs

Test organism	Conc. per well (μg)	Zone of inhibition (mm)		MIC (mg/mL)		MBC (mg/mL)		MFC (mg/mL)	
		A	E	A	E	A	E	A	E
<i>S. aureus</i>	50	10	8	0.250	0.5	0.5	0.625	0.5	0.625
	100	12	10						
<i>B. subtilis</i>	50	9	N.A.	0.250	N.A.	0.5	N.A.	0.5	N.A.
	100	12	N.A.						
<i>E. coli</i>	50	13	8	0.0625	0.250	0.5	0.625	0.5	0.625
	100	15	10						
<i>P. aeruginosa</i>	50	10	7	0.250	0.5	0.5	0.625	0.5	0.625
	100	13	10						
<i>K. pneumoniae</i>	50	9	6	0.250	0.5	0.5	0.625	0.5	0.625
	100	11	8						
<i>A. niger</i>	50	10	7	0.250	0.5	0.5	0.625	0.5	0.625
	100	12	10						
<i>C. albicans</i>	50	9	8	0.125	0.250	0.5	0.625	0.5	0.625
	100	11	10						

A: AgNPs synthesized using *M. zapota*; and E: *M. zapota* fruit extract.

antimicrobial activity of AgNPs was better compared to that of the plant extract. The bactericidal effect of AgNPs could be due to the formation of positively charged Ag^+ ions, which interact with the thiol groups of proteins to restrict membrane permeability and inactivate essential enzymes, resulting in cell death. When AgNPs (Ag^0) are exposed to water or another oxidizing agent, they oxidize to silver ions (Ag^+), which are extremely poisonous to bacteria and best explain AgNPs' chemical mechanism. As a result, the small particle size of AgNPs exposes more surface area to water, resulting in a large number of silver ions (Ag^+) being produced, which then deactivate proteins required for bacterial viability [43].

Drug-excipient compatibility studies

The formulation work was preceded by preformulation studies which include drug excipient compatibility analysis. The same was assessed using FT-IR analysis. As observed from Figs. 12 and 13, no major changes were reported in the position of the major peaks produced in the AgNPs alone and in a mixture of AgNPs and carbopol in the FT-IR spectra, indicating that there was no interaction between the AgNPs and carbopol. Following which, two gel formulations were successfully prepared from the synthesized AgNPs using carbopol 934 (A) and carbopol 940 (C). Tables 6 and 7 report the

transmittance values corresponding to the common functional groups present in MZ-AgNPs, carbopol 934, carbopol 940, and their mixture.

Formulation of AgNPs incorporated gels

Two gel formulations were successfully prepared with carbopol 934 and carbopol 940 gel bases.

Evaluation of gels

Color, appearance, and homogeneity

The controls carbopol 934 and carbopol 940 were translucent and colorless, whereas AgNPs incorporated gel formulations A and C were brownish in color, free from lumps and foreign particles and homogeneous in nature.

pH and viscosity

The gels were almost neutral with pH values between 6.27 ± 0.07 and 7.00 ± 0.00 . The viscosity of gels A, C, and M was found to be 16.76, 91.53, and 86.12 Pa·s, respectively. Viscosity reflects consistency. Viscosity of gel C containing carbopol 940 was much higher than that of gel A containing carbopol 934 and was closer to the marketed gel M. Results are reported in Table 8.

Spreadability

Spreadability reflects the size of the area across

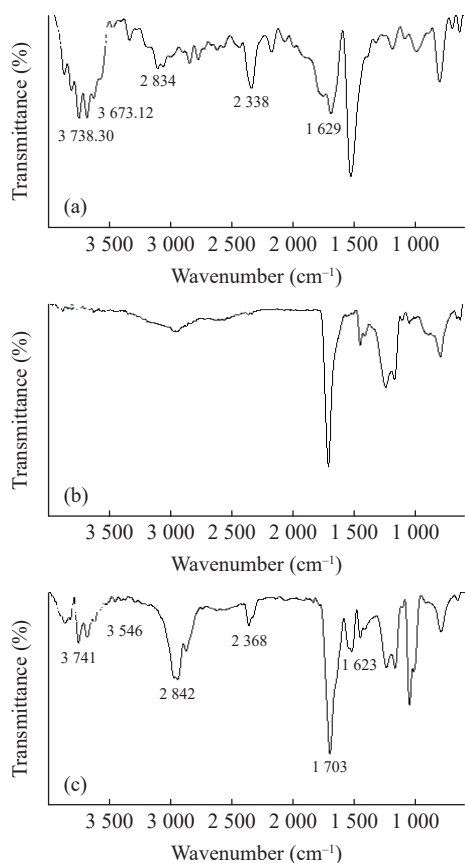


Fig. 12 FT-IR spectra of (a) pure MZ-AgNPs, (b) carbopol 934, and (c) mixture of carbopol 934 and MZ-AgNPs.

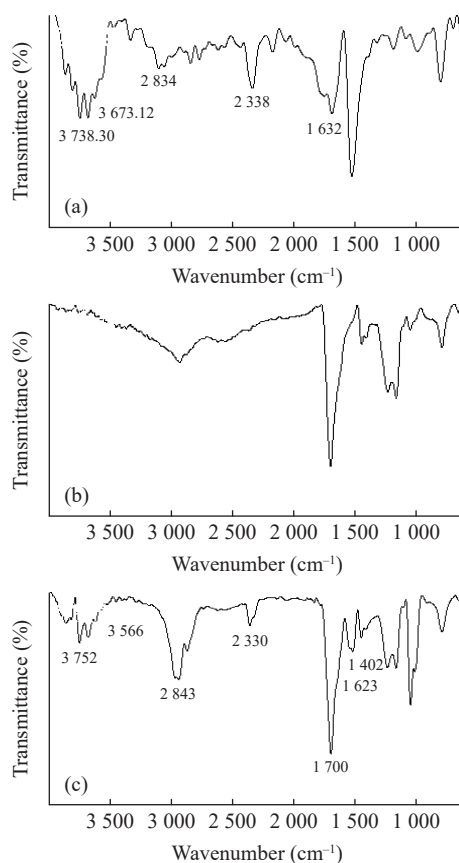


Fig. 13 FT-IR spectra of (a) pure MZ-AgNPs, (b) carbopol 940, and (c) mixture of carbopol 940 and MZ-AgNPs.

Table 6 Transmittance values corresponding to the common functional groups present in MZ-AgNPs, carbopol 934, and their mixture

Functional groups	Transmittance (cm ⁻¹)
H-bonded O—H, amino acid (NH ₃ ⁺), carboxylic acid (O—H)	3 400–3 800
Aliphatic C—H	2 834, 2 842
Isocyanate (stretch), S—H (stretch), N—H (amino acid)	2 338–2 368
C=O	1 700, 1 708, 1 703
N—H bending	1 623, 1 629

Table 7 Transmittance values corresponding to the common functional groups present in MZ-AgNPs, Carbopol 940, and their mixture

Functional groups	Transmittance (cm ⁻¹)
3 200–3 600	H-bonded O—H, amino acid, carboxylic acid
3 000–3 100	Alkene C—H, aromatic C—H
2 834, 2 843	Aliphatic C—H
2 338, 2 330	Isocyanate, S—H, N—H
1 700, 1 699	C=O
1 632, 1 623	N—H bending
1 520, 1 523	N—H bending, Alkene(C=C), Aromatic(C=C)
1 448, 1 402	C—O—H bending, C—N stretching, C—O stretching

Table 8 Extrudability of AgNPs gel formulations A and C and marketed formulation M

Gel	Extrudability	pH	Viscosity (Pa·s)	Spreadability (cm)	Zeta potential (mV)
A	31.13 ± 0.05	6.27 ± 0.07	16.76 ± 0.11	1.61 ± 0.06	-35.70 ± 0.00
C	29.79 ± 0.36	6.25 ± 0.13	91.53 ± 0.05	1.52 ± 0.05	-31.40 ± 0.00
M	30.23 ± 0.15	7.00 ± 0.00	86.12 ± 0.02	1.59 ± 0.04	-36.45 ± 0.00

which the gel spreads easily when applied to the skin/affected part. It is a crucial property for uniform application of gel to a greater region of skin, which provides a good patient compliance. The therapeutic potency is also influenced by the value spread. The spreadability of the formulated gels was closer to the marketed formulation. The spreadability of gel A was better compared to that of gel C. Table 8 shows the results.

Zeta potential

The formulations showed high zeta potential values between -31.40 and -36.45 mV (Table 8), indicating high stability. The generated silver nanoparticle loaded gel has enough charge and mobility to prevent nanoparticle aggregation. For silver nanoparticle laden gel, zeta potential was shown to be negative. The fact that the zeta potential is negative indicates that nanoparticles are stable against aggregation. Negatively charged particles repel one another in a nanoparticulate solution, causing them to behave as independent entities.

Extrudability

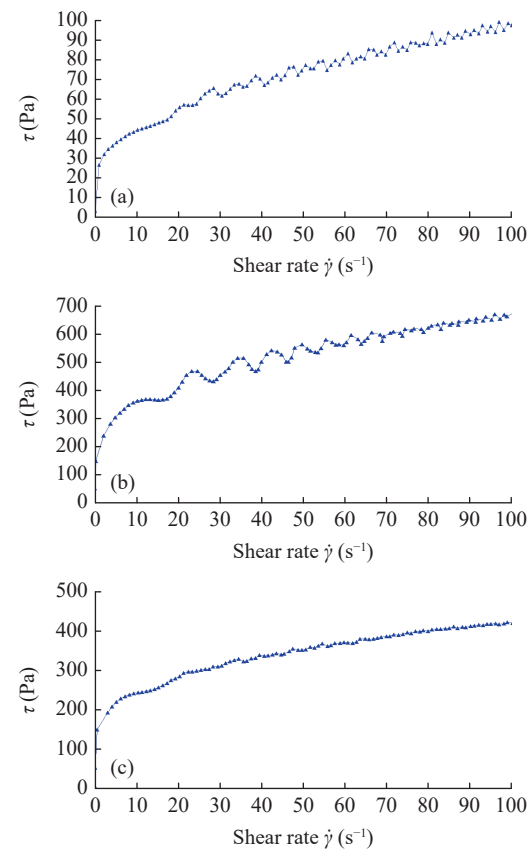
Extrudability of the gel from the tube is crucial for its applicability. Highly viscous gels may not easily extrude out from the tube, but low viscosity gels may flow quickly, necessitating the use of a consistency that allows the gel to be extruded from the tube [20]. The formulated gels showed an extrudability approaching that of the marketed formulation and the extrudability of gel A was better than that of gel C (Table 8).

Rheological studies

With increasing shear rate, all of the formulations showed a decrease in viscosity (shear thinning behavior), providing the gels good spreadability.

Steady shear properties

Figure 14 shows the graph between shear stress versus shear rate. It can be seen from the graph that with increasing rate of shear, stress increases and viscosity of the gel decreases. This revealed shear

**Fig. 14** Graph of shear stress (τ) versus γ of AgNPs gel formulations A and C and marketed formulation M

thinning behavior of the formulated gels. The values of τ , K , n , and R^2 were obtained from the graph and are reported in Table 9. K ranged between 16.76 and 146.01 Pa·s, where A showed the least and M showed the highest value. K denoted viscous behavior. If the value of $n = 1$, the system exhibits Newtonian fluid behavior and if the value of $n > 1$, then the system is said to have a thickening behavior. The n value for the gels ranged between 0.24 and 0.39, and hence the gel formulations showed a thinning behavior upon shearing and represented non-Newtonian fluid. The R^2

Table 9 Yield stress, consistency, flow index, and R^2 values of AgNPs gel formulations A and C and marketed formulation M

Formulation	τ (Pa)	K (Pa·s)	n	R^2
A	3.02	16.76	0.37 (shear thinning)	0.986
C	116.79	91.5	0.39 (shear-thinning)	0.971
M	146.01	146.01	0.24 (shear-thinning)	0.987

values for the equations were greater than 0.971, indicating that the power law findings were best fit. K can also be utilized as viscosity criteria [44].

Frequency sweep test

More direct correlation with the microstructure of gels can be provided by dynamic rheology compared to steady rheology as it provides for the materials to be examined in their at-rest state without disrupting their structures [45]. The viscoelastic behavior of the gels is illustrated in Fig. 15 using frequency sweep test at 25 °C, which shows the graph between G' and G'' . The data obtained from frequency sweep test revealed that the gels are viscoelastic in nature.

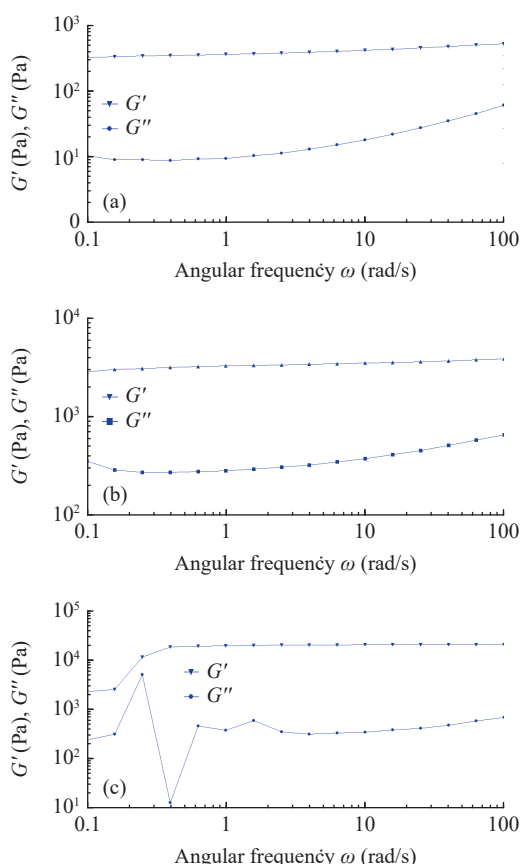


Fig. 15 Frequency dependence data of AgNPs gel formulations A and C and marketed formulation M at 37 °C.

In vitro diffusion

The cumulative drug release (AgNPs) after 8 h is reported in Table 10 and was found to be 80.03% and 78.78% for gels A and C, respectively.

Release kinetic studies

The data from the release of AgNPs from gel formulations was fitted to a variety of kinetic equations, including zero order, first order, Higuchi model, and Korsmeyer-Peppas model. Table 11

Table 10 Cumulative drug release of gel formulations A & C with time

Serial No.	Time (h)	Cumulative drug release (%)	
		A	C
1	0	2.1	1.5
2	0.5	3.9	2.6
3	1	11.23	10.1
4	2	19.45	18.21
5	3	29.12	27.99
6	4	43.43	42
7	5	51.22	50.13
8	6	53.15	52
9	7	68.01	67.11
10	8	80.03	78.78

Table 11 R^2 values for different equations and models

Formulation	Zero order	First order	Higuchi model	Korsmeyer-Peppas model
A	0.990	0.933	0.915	0.896
C	0.989	0.936	0.906	0.866

displays the results obtained. The results show that the release of AgNPs from gel formulations follows zero order kinetics, as evidenced by greater R^2 values in zero order kinetics. Also, R^2 value for gel A was higher compared to gel C, indicating more linear drug release from gel A.

Stability studies

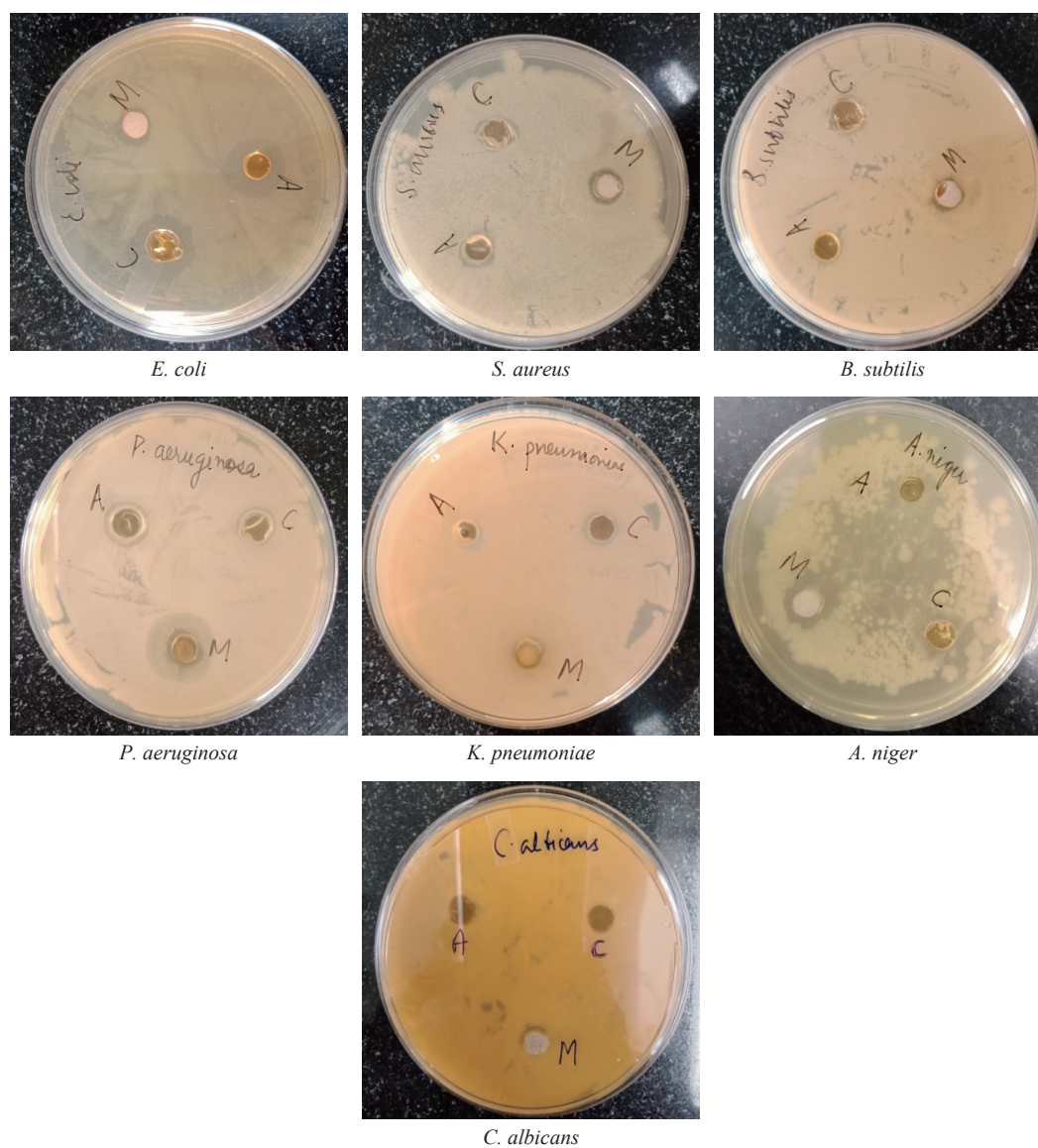
The formulated gels were physically and chemically stable for more than 6 months. No changes were observed in the color, appearance, pH, and zeta potential of the AgNPs gel formulations even after 6 months.

Antimicrobial activity of AgNPs gel formulations

From the results (Table 12 and Fig. 16), it can be seen that the antimicrobial activity of the gel (0.055% mass fraction) was comparable with the marketed formulation silverex containing 0.2% (mass fraction) silver nitrate. Moreover, in case of gram negative bacterium *E. coli*, the formulated gel reported greater zone of inhibition than the marketed formulation. Moderate activity was observed against *P. aeruginosa*, *A. niger*, and *S. aureus*. Least activity was observed against *B. subtilis*, *C. albicans* and *K. pneumoniae*. Hence, the formulated gel containing lesser dose of silver could serve as an effective alternative antimicrobial for the treatment of

Table 12 Antimicrobial activity of AgNPs gel formulations A and C and marketed formulation M

Test organism	Zone of inhibition (mm)		
	A	C	M
<i>S. aureus</i>	11	13	12
<i>B. subtilis</i>	10	12	10
<i>E. coli</i>	19	20	11
<i>P. aeruginosa</i>	13	11	20
<i>K. pneumoniae</i>	10	10	10
<i>A. niger</i>	14	15	15
<i>C. albicans</i>	10	10	10

**Fig. 16** Zone of inhibition of AgNPs gel formulations A and C and marketed formulation M against *E. coli*, *S. aureus*, *B. subtilis*, *P. aeruginosa*, *K. pneumoniae*, *A. niger*, and *C. albicans*.

pathogenic diseases caused by antibiotic resistant microbes. Silver nanoparticles exhibit their antimicrobial effect by protein inactivation, interference with DNA replication, and alteration in cell membrane permeability. Silver nanoparticles

have been shown to anchor in the bacterial cell wall and produce physical changes in the cell membrane, resulting in membrane damage and leakage of cellular contents [46]. The greater antibacterial action observed against *E. coli* could be attributed to the

difference in sensitivity and cell wall thickness between gram negative and Gram positive bacteria [47].

Conclusion

The topical gels incorporated with the optimized AgNPs biosynthesized using *M. zapota* fruit extract exert broad spectrum antimicrobial activity, which could lead to a promising alternative for treating pathogenic infections.

CRedit Author Statement

Sonia Parashar: Data curation, investigation, methodology, writing–review and editing, and formal analysis. **Munish Garg:** Conceptualization, project administration, and supervision.

Acknowledgement

The research has been supported by University Research Scholarship (URS) awarded to author SP.

Conflict of Interest

The authors declare that no competing personal or financial interest exists.

References

- [1] G. Kapoor, S. Saigal, A. Elongavan. Action and resistance mechanisms of antibiotics: A guide for clinicians. *Journal of Anaesthesiology, Clinical Pharmacology*, 2017, 33(3): 300–305. https://doi.org/10.4103/joacp.JOACP_349_15
- [2] S. Parashar, M.K. Sharma, C. Garg, et al. Green synthesized silver nanoparticles as silver lining in antimicrobial resistance: A review. *Current Drug Delivery*, 2022, 19(2): 170–181. <https://doi.org/10.2174/1567201818666210331123022>
- [3] Y. Wu, Y. Yang, Z. Zhang, et al. A facile method to prepare size-tunable silver nanoparticles and its antibacterial mechanism. *Advanced Powder Technology*, 2018, 29(2): 407–415. <https://doi.org/10.1016/j.apt.2017.11.028>
- [4] X.F. Zhang, Z.G. Liu, W. Shen, et al. Silver nanoparticles: Synthesis, characterization, properties, applications, and therapeutic approaches. *International Journal of Molecular Sciences*, 2016, 17(9): 1534. <https://doi.org/10.3390/ijms17091534>
- [5] A. Husen, K.S. Siddiqi. Phytosynthesis of nanoparticles: Concept, controversy and application. *Nanoscale Research Letters*, 2014, 9(1): 229. <https://doi.org/10.1186/1556-276X-9-229>
- [6] A. Kunhikrishnan, H.K. Shon, N.S. Bolan, et al. Sources, distribution, environmental fate, and ecological effects of nanomaterials in wastewater streams. *Critical Reviews in Environmental Science and Technology*, 2015, 45(4): 277–318. <https://doi.org/10.1080/10643389.2013.852407>
- [7] M. Hasan, K. Mehmood, G. Mustafa et al. Phytotoxic evaluation of phytosynthesized silver nanoparticles on lettuce. *Coatings*, 2021, 11(2): 225. <https://doi.org/10.3390/coatings11020225>
- [8] M. Hasan, A. Zafar, M. Imran, et al. Crest to trough cellular drifting of green-synthesized zinc oxide and silver nanoparticles. *ACS Omega*, 2022, 7(39): 34770–34778. <https://doi.org/10.1021/acsomega.2c02178>
- [9] S.O. Aisida, K. Ugwu, P.A. Akpa, et al. Biogenic synthesis and antibacterial activity of controlled silver nanoparticles using an extract of *Gongronema Latifolium*. *Materials Chemistry and Physics*, 2019, 237: 121859. <https://doi.org/10.1016/j.matchemphys.2019.121859>
- [10] N. Madubuonu, S.O. Aisida, I. Ahmad, et al. Bio-inspired iron oxide nanoparticles using Psidium guajava aqueous extract for antibacterial activity. *Applied Physics A*, 2020, 126(1): 1–8. <https://doi.org/10.1007/s00339-019-3249-6>
- [11] M. Hasan, J. Iqbal, U. Awan, et al. Mechanistic study of silver nanoparticle's synthesis by dragon's blood resin ethanol extract and antiradiation activity. *Journal of Nanoscience and Nanotechnology*, 2015, 15(2): 1320–1326. <https://doi.org/10.1166/jnn.2015.9090>
- [12] J.M. Ahn, H.J. Eom, X. Yang, et al. Comparative toxicity of silver nanoparticles on oxidative stress and DNA damage in the nematode. *Caenorhabditis elegans. Chemosphere*, 2014, 108: 343–352. <https://doi.org/10.1016/j.chemosphere.2014.01.078>
- [13] L. Maurer, J.N. Meyer. A systematic review of evidence for silver nanoparticle-induced mitochondrial toxicity. *Environmental Science: Nano*, 2016, 3(2): 311–322. <https://doi.org/10.1039/C5EN00187K>
- [14] O.S. Adeyemi, E.O. Shittu, O.B. Akpor, et al. Silver nanoparticles restrict microbial growth by promoting oxidative stress and DNA damage. *EXCLI Journal*, 2020, 19: 492–500. <https://doi.org/10.17179/excli2020-1244>
- [15] S.K. Kailasa, T.J. Park, J.V. Rohit, et al. Antimicrobial activity of silver nanoparticles. *Nanoparticles in pharmacotherapy*. Amsterdam: Elsevier, 2019: 461–484. <https://doi.org/10.1016/B978-0-12-816504-1.00009-0>
- [16] D.A. Helal, D.A. El-Rhman, S.A. Abdel-Halim, et al. Formulation and evaluation of fluconazole topical gel. *International Journal of Pharmacy and Pharmaceutical Sciences*, 2012, 4(SUPPL. 5): 176–183.
- [17] H.J. Rathod, D.P. Mehta. A review on pharmaceutical gel. *International Journal of Pharmaceutical Sciences*, 2015, 1(1): 33–47.
- [18] R.M.P. Singh, A. Kumar, K. Pathak. Thermally triggered mucoadhesive *in situ* gel of loratadine: β -cyclodextrin complex for nasal delivery. *AAPS PharmSciTech*, 2013, 14(1): 412–424. <https://doi.org/10.1208/s12249-013-9921-9>
- [19] R.S. dos Santos, H.C. Rosseto, J.B. da Silva, et al. The effect of carbomer 934P and different vegetable oils on physical stability, mechanical and rheological properties of emulsion-based systems containing propolis. *Journal of Molecular Liquids*, 2020, 307: 112969. <https://doi.org/10.1016/j.molliq.2020.112969>
- [20] S. Chanda, R. Nair. Antimicrobial activity of *Terminalia catappa*, *Manilkara zapota* and *Piper betel* leaf extract. *Indian Journal of Pharmaceutical Sciences*, 2008, 70(3): 390–393.
- [21] M.H. Ibraheim, A.A. Ibrahiem, T.R. Dalloul. Biosynthesis of silver nanoparticles using Pomegranate juice extract and its antibacterial activity. *International Journal of Applied Sciences and Biotechnology*, 2016, 4(3): 254–258. <https://doi.org/10.3126/ijasbt.v4i3.15417>

- [22] N. Swilam, K.A. Nematallah. Polyphenols profile of pomegranate leaves and their role in green synthesis of silver nanoparticles. *Scientific Reports*, 2020, 10: 14851. <https://doi.org/10.1038/s41598-020-71847-5>
- [23] W.L. Zhang, W.B. Jiang. Antioxidant and antibacterial chitosan film with tea polyphenols-mediated green synthesis silver nanoparticle via a novel one-pot method. *International Journal of Biological Macromolecules*, 2020, 155: 1252–1261. <https://doi.org/10.1016/j.ijbiomac.2019.11.093>
- [24] P.K. Tyagi, S. Tyagi, D. Gola, et al. Ascorbic acid and polyphenols mediated green synthesis of silver nanoparticles from tagetes erecta L. aqueous leaf extract and studied their antioxidant properties. *Journal of Nanomaterials*, 2021, 2021: 1–9. <https://doi.org/10.1155/2021/6515419>
- [25] P. Moteriya, H. Padalia, S. Chanda. Characterization, synergistic antibacterial and free radical scavenging efficacy of silver nanoparticles synthesized using Cassia roxburghii leaf extract. *Journal of Genetic Engineering and Biotechnology*, 2017, 15(2): 505–513. <https://doi.org/10.1016/j.jgeb.2017.06.010>
- [26] S. Mathew, C.P. Victorio, J. Sidhi. Biosynthesis of silver nanoparticle using flowers of *Calotropis gigantea* (L.) W.T. Aiton and activity against pathogenic bacteria. *Arabian Journal of Chemistry*, 2020, 13(12): 9139–9144. <https://doi.org/10.1016/j.arabjc.2020.10.038>
- [27] D. Elumalai, M. Hemavathi, C.V. Deepaa, et al. Evaluation of phytosynthesized silver nanoparticles from leaf extracts of *Leucas aspera* and *Hyptissuaveolens* and their larvicidal activity against malaria, dengue and filariasis vectors. *Parasite epidemiology and control*, 2017, 2(4): 15–26.
- [28] R.C. Murdock, L. Braydich-Stolle, A.M. Schrand, et al. Characterization of nanomaterial dispersion in solution prior to *in vitro* exposure using dynamic light scattering technique. *Toxicological Sciences*, 2008, 101(2): 239–253. <https://doi.org/10.1093/toxsci/kfm240>
- [29] P.R. Murray, E.J. Baron. *Manual of clinical microbiology*. 8th ed. Washington: ASM Press, 2003.
- [30] J.C. Ontong, S. Singh, O.F. Nwabor, et al. Potential of antimicrobial topical gel with synthesized biogenic silver nanoparticle using *Rhodomyrtus tomentosa* leaf extract and silk sericin. *Biotechnology Letters*, 2020, 42(12): 2653–2664. <https://doi.org/10.1007/s10529-020-02971-5>
- [31] K. Singh, M. Panghal, S. Kadyan, et al. Evaluation of antimicrobial activity of synthesized silver nanoparticles using *phyllanthus amarus* and *tinospora cordifolia* medicinal plants. *Journal of Nanomedicine & Nanotechnology*, 2014, 5(6): 1000250. <https://doi.org/10.4172/2157-7439.1000250>
- [32] M. Shukr, G.F. Metwally. Evaluation of topical gel bases formulated with various essential oils for antibacterial activity against methicillin-resistant *Staphylococcus aureus*. *Tropical Journal of Pharmaceutical Research*, 2014, 12(6): 877. <https://doi.org/10.4314/tjpr.v12i6.3>
- [33] G. Misal, G. Dixit, V. Gulkari. Formulation and evaluation of herbal gel. *Indian Journal of Natural Products and Resources*, 2012, 3(4): 501–505.
- [34] K.S. Sandhu, N. Singh, M. Kaur. Characteristics of the different corn types and their grain fractions: Physicochemical, thermal, morphological, and rheological properties of starches. *Journal of Food Engineering*, 2004, 64(1): 119–127. <https://doi.org/10.1016/j.jfoodeng.2003.09.023>
- [35] S. Park, M.G. Chung, B. Yoo. Effect of octenylsuccinylation on rheological properties of corn starch pastes. *Starch*, 2004, 56(9): 399–406. <https://doi.org/10.1002/star.200300274>
- [36] E.J. Ricci, M.V. Bentley, M. Farah, et al. Rheological characterization of poloxamer 407 lidocaine hydrochloride gels. *European Journal of Pharmaceutical Sciences*, 2002, 17(3): 161–167. [https://doi.org/10.1016/S0928-0987\(02\)00166-5](https://doi.org/10.1016/S0928-0987(02)00166-5)
- [37] A. Prusty, P. Parida. Development and evaluation of gel incorporated with biogenically synthesised silver nanoparticles. *Journal of Applied Biopharmaceutics and Pharmacokinetics*, 2015, 3(1): 1–6. <https://doi.org/10.14205/2309-4435.2015.03.01.1>
- [38] S. Dash, P.N. Murthy, L. Nath, et al. Kinetic modeling on drug release from controlled drug delivery systems. *Acta Poloniae Pharmaceutica*, 2020, 67(3): 217–223.
- [39] N. Mahendran, B. Anand, M. Rajarajan, et al. Green synthesis, characterization and antimicrobial activities of silver nanoparticles using *Cissus quadrangularis* leaf extract. *Materials Today: Proceedings*, 2021, 49(7): 2620–2623. <https://doi.org/10.1016/j.matpr.2021.08.043>
- [40] K.Y. Yong, M.S. Abdul Shukkoor. Manilkara Zapota: A phytochemical and pharmacological review. *Materials Today: Proceedings*, 2020, 29: 30–33. <https://doi.org/10.1016/j.matpr.2020.05.688>
- [41] H. Erjaee, H. Rajaian, S. Nazifi. Synthesis and characterization of novel silver nanoparticles using *Chamaemelum nobile* extract for antibacterial application. *Advances in Natural Sciences: Nanoscience and Nanotechnology*, 2017, 8(2): 025004. <https://doi.org/10.1088/2043-6254/aa690b>
- [42] P. Mathur, S. Jha, S. Ramteke, et al. Pharmaceutical aspects of silver nanoparticles. *Artificial Cells, Nanomedicine, and Biotechnology*, 2018, 46(sup1): 115–126. <https://doi.org/10.1080/21691401.2017.1414825>
- [43] M. Sikora, S. Kowalski, P. Tomasik, et al. Rheological and sensory properties of dessert sauces thickened by starch-xanthan gum combinations. *Journal of Food Engineering*, 2007, 79(4): 1144–1151. <https://doi.org/10.1016/j.jfoodeng.2006.04.003>
- [44] B.L. Karwasra, B.S. Gill, M. Kaur. Rheological and structural properties of starches from different Indian wheat cultivars and their relationships. *International Journal of Food Properties*, 2017, 20(sup1): S1093–S1106. <https://doi.org/10.1080/10942912.2017.1328439>
- [45] M.P. Mishra, R.N. Padhy. Antibacterial activity of green silver nanoparticles synthesized from *Anogeissus acuminata* against multidrug resistant urinary tract infecting bacteria *in vitro* and host-toxicity testing. *Journal of Applied Biomedicine*, 2018, 16(2): 120–125. <https://doi.org/10.1016/j.jab.2017.11.003>
- [46] B. Khalandi, N. Asadi, M. Milani, et al. A review on potential role of silver nanoparticles and possible mechanisms of their actions on bacteria. *Drug Research*, 2016, 67(2): 70–76. <https://doi.org/10.1055/s-0042-113383>
- [47] Y. Qing, L. Cheng, R. Li, et al. Potential antibacterial mechanism of silver nanoparticles and the optimization of orthopedic implants by advanced modification technologies. *International Journal of Nanomedicine*, 2018, 13: 3311–3327. <https://doi.org/10.2147/IJN.S165125>

© The author(s) 2023. This is an open-access article distributed under the terms of the Creative Commons Attribution 4.0 International License (CC BY) (<http://creativecommons.org/licenses/by/4.0/>), which permits unrestricted use, distribution, and reproduction in any medium, provided the original author and source are credited.